京 都 大 学 防 災 研 究 所 年 報　第47号 C　平成16年3月
Annuals of Disas. Prev. Res. Inst., Kyoto Univ., No. 47 C, 2004

Advanced Techniques for Evaluating Vulnerability of Urban Infrastructure by Integrating Multiple Evaluation Indexes

Tadanobu SATO, Kojiro IRIKURA, Masayoshi NAKASHIMA, Hitoshi TANAKA,
Kouji MATSUNAMI, Sumio SAWADA, Keiichiro SUITA,
Tomotaka IWATA and Riki HONDA

Synopsis

It is essential for disaster prevention to quantitatively evaluate the earthquake vulnerability of urban infrastructures considering the duration of infrastructures in service, external loads to act on structure during earthquakes, cost of damage and restoration, and the cost of maintenance and retrofitting. For this purpose, we propose an integrated methodology that covers the prediction of strong ground motions for scenario earthquakes, control of structural damage of RC and steel building structures and evaluation of residual seismic performance after damage, and estimation of life cycle cost-based maintenance strategies.

Keywords: strong ground motion prediction, characterized source model, seismic rehabilitation, seismic performance estimation, full-scale experiment, life cycle cost

1. Introduction

To evaluate earthquake vulnerability of urban infrastructures we have to develop techniques for evaluating (1) life time of infrastructures, (2) external input to structure during event occurrences, (3) cost of damage to infrastructures and restoration cost, (4) maintenance and retrofit cost. For this purpose we are conducting researches on prediction of strong ground motions for scenario earthquakes, and control of structural damage to RC and steel building structures subjected to earthquakes and evaluation of residual seismic performance after damage.

In the first research subject we are constructing a framework of strong ground motion prediction using a characterized source model and underground structure model for scenario earthquakes. Estimated strong ground motions can be used for evaluation of structure damages.

The second research subject aims to develop a systematic method to diagnose the seismic performance of building stock in urban areas spread throughout Japan. This provides information essential for the policy making and practical technologies on rehabilitation and renewal of urban infrastructures, maintenance of large building stock, and development of sustainable urban societies.

Based on these researches we propose methodologies for prioritization seismic reinforcement of existing infrastructures based on the

concept of Life Cycle Cost taking into account seismic risk. Because LCC is defined as the expected total cost during a planned service time of a structure which include the costs of plan, design, construction, maintenance, repair and dismantlement we can optimize seismic reinforcement and maintenance plan of existing infrastructures.

2. Strong Ground Motion Prediction for Design Ground Motion

The M8-class subduction earthquakes have occurred repeatedly in the Nankai trough. The headquarters for earthquake promotion reported that long-term evaluations of occurrence potentials of the next earthquakes (Nankai and Tonankai) at the trough are from 40% to 50% within 30 years from 2001. Moreover, in Kanai area, crustal earthquakes, such as the 1995 Kobe earthquake, the 2000 Tottori-ken seibu earthquake are seems to occur in the second half period between the subduction earthquakes. Therefore, strong ground motion prediction for the scenario earthquakes is a important issue for seismic disaster mitigation.

From lessons of the 1995 Hyogoken-Nanbu (Kobe) earthquakes, we have learned that estimation of near-source ground motions is quite important for mitigation of seismic disasters. Methods to predict strong ground motions in a quantitative manner will be developed (Irikura and Miyake, 2001, Irikura et al., 2004). Both theoretical and semi-empirical approaches are applied taking into account the physical and geometrical properties of earthquake faults and seismic wave propagation characteristics of the crust and surface geology. Source and propagation-path characterizations are important issues for simulating ground motions. In this chapter, we will explain some analysis for improvement of source and propagation-path modelings.

2.1 Dynamic source parameters for the source characterization

It is one of the important issues to construct the appropriate source model for strong motion prediction of scenario earthquakes. Recent dense strong motion network data enable us to analyze detail source rupture process of destructive earthquakes. Obtained source rupture processes were heterogeneous and those heterogeneities control near-source strong ground motions. Somerville et al. (1999) characterized source slip model of mainly California earthquakes from strong motion waveform inversion. They defined asperity which is an area whose final slip is larger than 1.5 times of average slip value. They found total asperity size is followed by a scaling relation. Recent events such as the 2000 Tottori-ken Seibu earthquake, the 1999 Chichi, Taiwan, and Kocaeli, Turkey, and other moderate-size crustal earthquakes are found to follow the relation (Miyakoshi et al., 2000). Irikura and Miyake (2001) proposed characterized source model based on this scaling relation for strong motion prediction. The availability of the characterized source models has been proved through the strong motion simulation in near-source area in the broadband frequency band (BB) for e.g., the 1995 Kobe (Kamae and Irikura, 1998) and for the 2000 Tottoriken-Seibu (Ikeda et al., 2002) earthquakes.

In those simulations, they assumed stress drops only for the asperities by forward simulation of the high frequency contents of the records. When constructing a characterized source model for BB strong motion, we need rules to set stress parameters. We examine dynamic source parameters such as stress parameters by mapping method of spatio-temporal shear-stress distribution on the fault

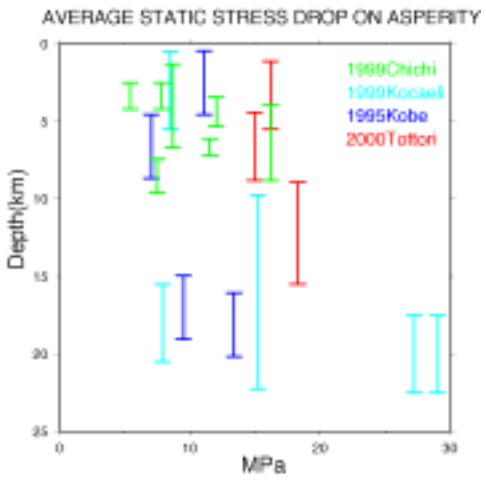

Fig.1 Depth dependence of static stress drop parameters on the asperities for four earthquakes (Iwata et al., 2004)

plane from a spatio-temporal slip distribution from kinematic waveform inversion (e.g., Bouchon, 1997; Zhang et al., 2003). Dynamic source parameters averaged over on- and off-asperity areas are estimated from a viewpoint of characterized source model. Average effective stress values of on- and off-asperity areas are estimated as 10-20MPa and about 5MPa. Stress parameters on the asperities seem to be increasing with asperity depth. Fig. 1 shows depth dependence of static stress drops at the asperities for four earthquakes. Stress parameters on the asperities coincide with the ones that were used for forward ground motion modeling (e.g. Kamae and Irikura, 2002, Ikeda et al., 2002). Characterization of stress parameters contributes the development of characterized source model.

2.2 Construction of underground structure model using long-period ground motion simulation

We have developed the crustal structure model from the source region of the Nankai trough to the Osaka basin in Kinki area for ground motion modeling by comparing observed records and simulated long-period (>2s) ground motions. Simulated S-wave ground motion records reproduced well by a constructed 3D underground structure model. We showed that this 3D structure model is applicable for the ground motion simulation in the long period range, however it is needed more detail crustal velocity structure information for a better

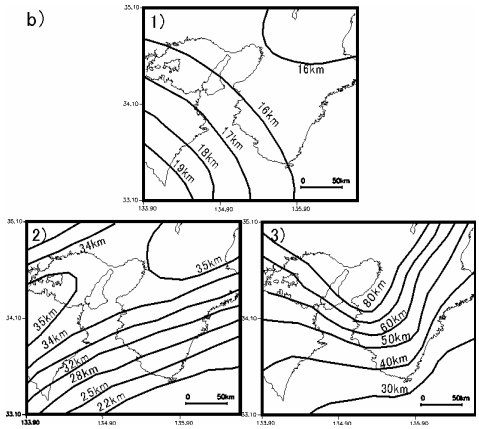

Fig.2 Contour map of the Conrad, Moho, and the upper bound of Philippine-Sea plate for the 3D underground structure model (Yamada and Iwata, 2004).

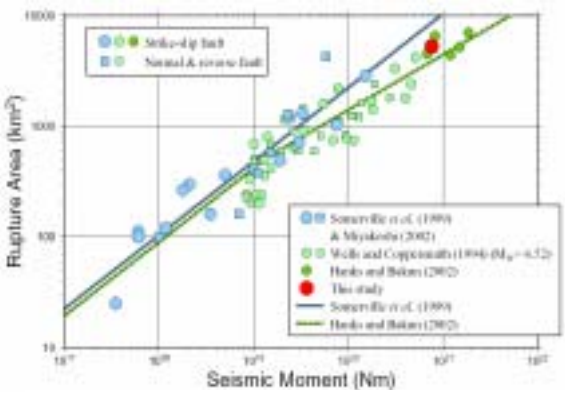

Fig.3 The relationship between seismic moment and rupture area (Asano et al., 2004)

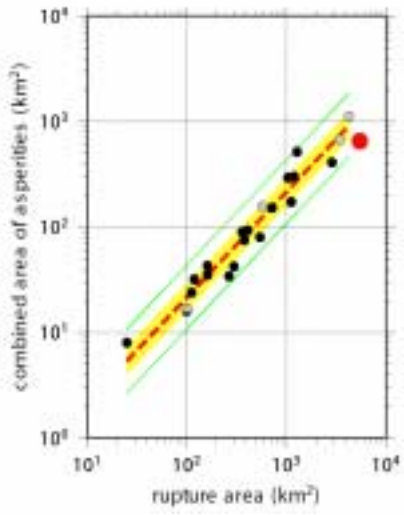

Fig.4 Relationship between rupture area and combined asperity area. The 2002 Denali earthquake is marked as the closed red on the relation of Irikura and Miyake(2001) (Asano et al., 2004)

Table 1 Results of UT inspection

building	location	Inspection	qualified	qualified(%)	defect
A	X1Y3(L3U)	18	0	0.0	64
	X1Y2(L4U)	16	1	6.3	31
	X2Y3(L5R)	18	5	27.8	39
	sub-total	52	6	11.5	134
B	X1Y1(L2R)	18	9	50.0	15
	X1Y2(T2R)	18	5	27.8	25
	X2Y1(L1U)	18	14	77.8	9
	X2Y2(T1U)	20	6	30.0	29
	sub-total	74	34	45.9	78
Total		126	40	31.7	212

reproduction of the whole observed records. In Fig. 2, the constructed underground structure model by Yamada and Iwata (2004). Analysis in detail can be referred to Yamada and Iwata (2004).

2.3 Source scaling of the M8 class earthquake

A slip characterized scaling relations (e.g. Somerville et al, 1999; Miyakoshi et al., 2000) are treating until Mw7.6 (Chichi, Taiwan) event. There are an occurrence potentials of M8 class inland earthquakes, that is historically the 1894 Nobi earthquake. A hypothetical event at Itoigawa-Shizuoka tectonic line is asuumed to be M8 class. Therefore that is an important subject to see the heterogeneous source scaling relation more than Mw7.6 events. M_W 7.9 inland crustal earthquake occurred at the Denali fault system, Alaska, on November 3, 2002 at 22:12 (UTC). Source process of the 2002 Denali earthquake is estimated by the multiple time-window linear kinematic waveform inversion using strong motion and GPS-measured static displacement data. The obtained source model could explain both the observed strong motion waveforms and GPS-measured static displacements. Large slips on the fault plane are observed at about 80 - 90km east and about 150 - 200km east from the hypocenter. These features are consistent with observed surface rupture information and the other inversion results using teleseismic body waves. We also observed some portions of the whole fault with more than 4.0km/s rupture propagation velocity that exceeds the shear-wave velocity of the source region. The relation between the rupture area and seismic moment of this earthquake seems to follow the bilinear *L*-model scaling rather than the self-similar source scaling model. Combined area size of asperities is a little smaller than that expected from the empirical scaling relationship with seismic moment developed by compiling source inversion results. Fig.3 shows the relationship between rupture area and seismic moment. This event fits L-model rather than self-similar model.

Fig. 4 shows the relation between rupture area and combined asperity area. The2002 Denali earthquake shows a smaller size ratio of the combined asperity area to total rupture area. These information is quite useful for constructing the source models of M8-class inland earthquakes. In detail, Asano et al.(2004) can be reffered.

2.4 Research plan in FY2004

In this chapter, we have explained some analysis results of source and underground structure models, that will be used for constructing scenario earthquake source and underground models. In FY2004, we are trying to simulate ground motions

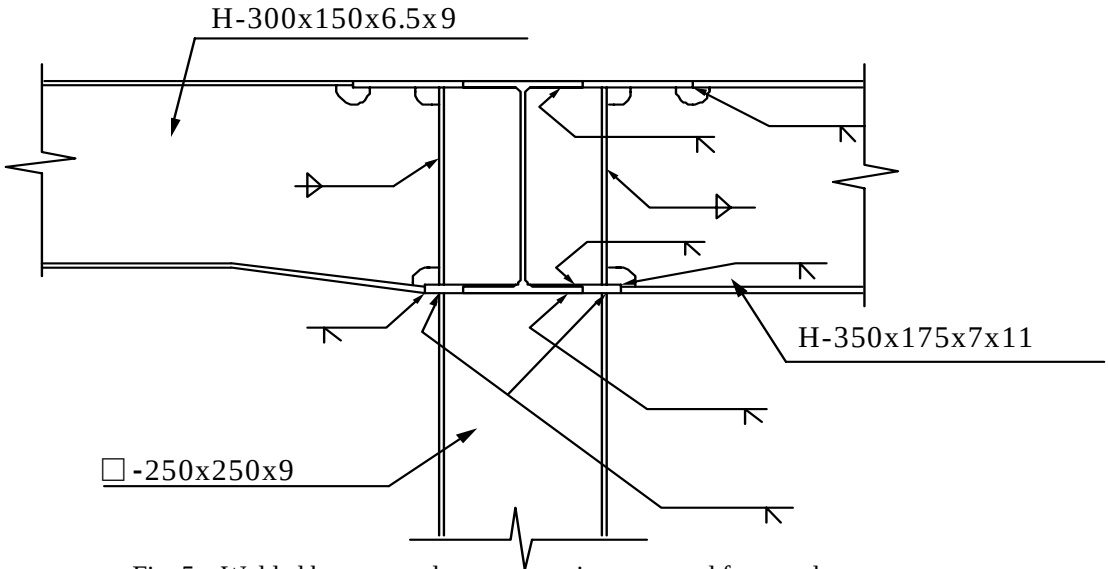

Fig. 5 Welded beam-to-column connection extracted from real structure

during some hypothetical earthquakes and discuss the effects of model parameters on ground motions.

3. Estimation of Seismic Performance of Buildings

3.1 Test on Seismic Performance of Welded Steel Joints of Twenty-five Years Old

One of the goals of this research project is to develop a simple and systematic procedure for estimating the seismic capacity of existing steel building structures. As an initial step to this goal, we conducted full-scale loading tests of welded beam-to-column subassemblages that were extracted from two real low-rise steel structures constructed in 1980 and 1981. This was the period of very rapid progress in steel construction, and present methods of welding and joining were being developed. This means that the subassemblages were the examples very useful for the evaluation of true seismic performance of the welded connections designed and constructed in the contemporary practices.

UT inspections were carried out for the two structures. As shown in Table 1, a total of 126 welded connections were inspected, and 212 weld defects were identified. The welds that were qualified comprised only 32 % of total. The difference between the two structures (Structures A and B) is also notable. In Structure A, the rate of qualification comprised only 11 % for Structure A, whereas the rate was 46 % for Structure B. This suggests the strong dependence of weld quality on workmanship. For the welded joints in which many defects were identified, portion of the joints were cut out, and macro tests were conducted to examine the true locations and severities of the weld related defects. A total of thirty welds included in twenty cross-sections were examined. Forty-six defects were disclosed, with the distribution with respect to the type of deflects given as nineteen locations for slug inclusion; six locations for fusion defects, ten locations for cracks, three locations for insufficient fusion, one location for brow hole, six locations for overlap, and one location for undercut. Comparison between UT inspection and the macro observation indicates that twenty-eight locations were identified accurately by UT inspection for the thirty-seven defects detected by the macro observation.

Fig. 5 shows one of the welded joints tested in this study. The tested joints consisted of a square tube of 250 mm by 250 mm for columns, and a wide-flange of 350 mm by 175 mm. Their thickness values were 9 mm for the tube column and 7 and 11 mm for the web and flanges of the wide-flange beams. Charpy V-notch tests were conducted for the beam materials of the tested connections. The results are shown in Fig. 6, indicating that the materials are very ductile even for

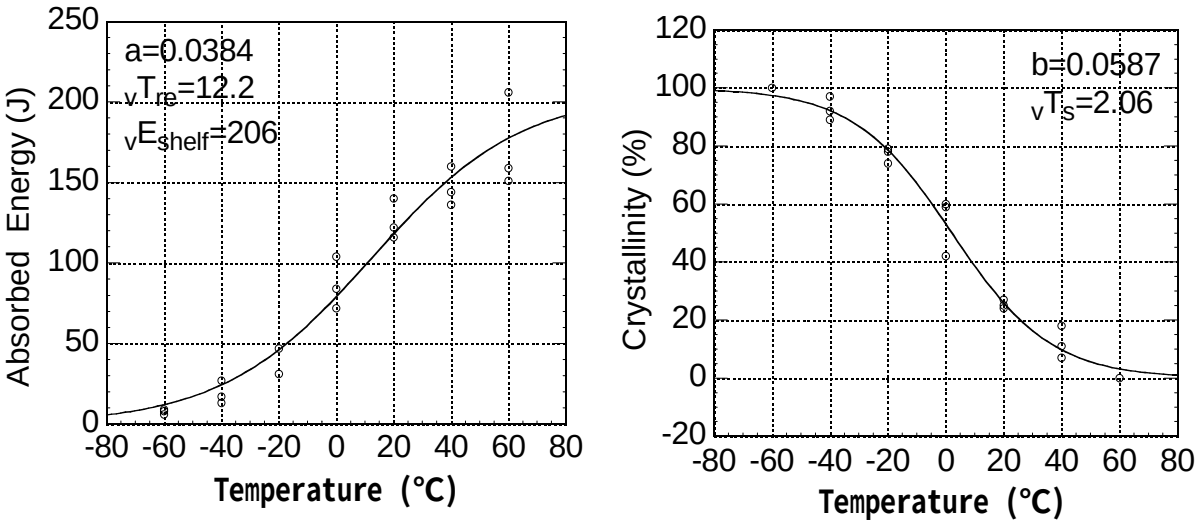

Fig. 6 Absorbed energy obtained from CVN tests

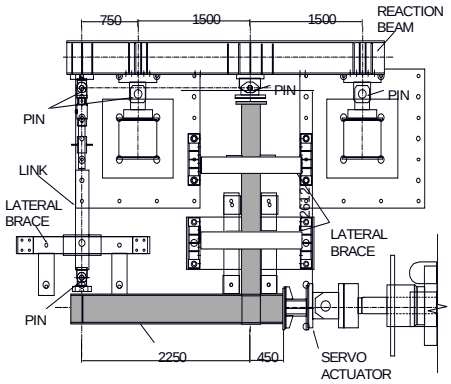

Fig. 7 Loading setup

the contemporary standards. The test setup and loading system is shown in Fig.7. Here, the loading actuator was installed at the free end of the beam. A standard loading protocol commonly used in Japan was adopted for the cyclic loading of the test specimen, i.e., two cycles of the yield rotation θ_y, $2\theta_y$, $3\theta_y$, and $4\theta_y$. Three specimens were tested, and the test results are presented in Fig. 10 in terms of the shear to the beam (normalized by the yield beam shear) and the beam chord angle. For all three specimens, for deformations whose chord angle was beyond 0.05 rad, flange local buckling occurred and the resistance decreased accordingly. For the specimen (L1U) in which no defect was detected from the UT inspection, a crack initiated from the toe of a lower flange's weld access hole, triggering the eventual fracture at the beam end. For the two specimens (L3U and L4U) in which defects were observed form the UT inspection, cracks started from the edge of the flange welds. In Specimen L3U, the location of crack initiation coincided with the location of the detected welds, while in Specimen L4U, the location was different from the location of the detected welds.

From the observations, the following conclusions are drawn.

(1) The steel material used in the early 1980s may be as ductile as the materials supplied in recent years.

(2) UT inspections are useful, but from the comparison between UT inspection and macro observation, the UT inspection's rate of success for the detection of weld defects are in the range of two-thirds.

(3) Although rather many defects were identified in the test specimens, overall ductility of the welded connections was rather good. A rotation capacity of 0.05 rad was ensured in all cases. One reason for such large ductility was a rather thin plate for the beam flanges.

3.2 Seismic Rehabilitation of Reinforced Concrete Frame Structures by Inserting Precast Concrete Panels

(1) Objectives

There exist a number of old apartment houses composed of reinforced concrete frame systems without having sufficient seismic resistant capacity. When an old apartment house does not have the seismic resistant capacity currently required by a national code, or AIJ (Architectural Institute of

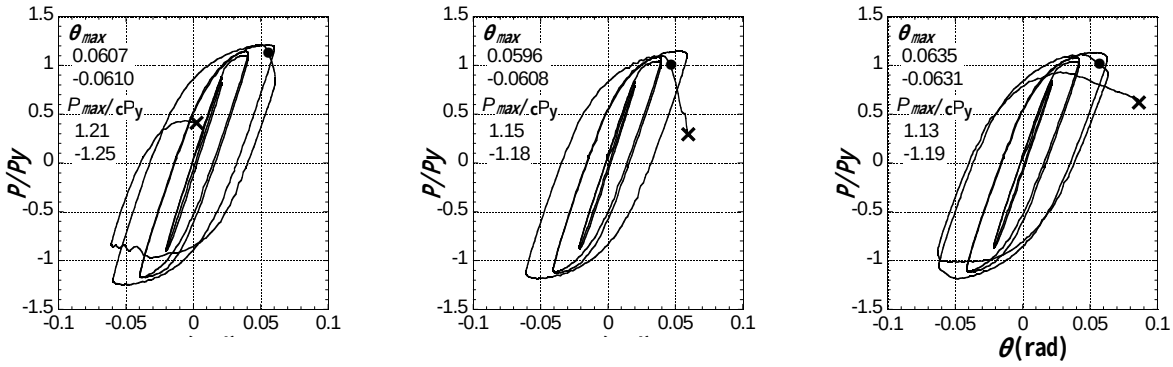

Fig.8 Force versus rotation relationship of tested connections: (a) L1U; (b) L3U; (c) L4U

Japan) code, ACI (American Concrete Institute)code, etc. , one of the solutions is to increase seismic resistant capacity of the frame structure by providing structural walls. In this study, it was experimentally and analytically shown that the seismic resistant capacity of a typical old frame structure for apartment houses can be enhanced to the currently required level by inserting precast concrete walls even without shear keys and dowel reinforcement.

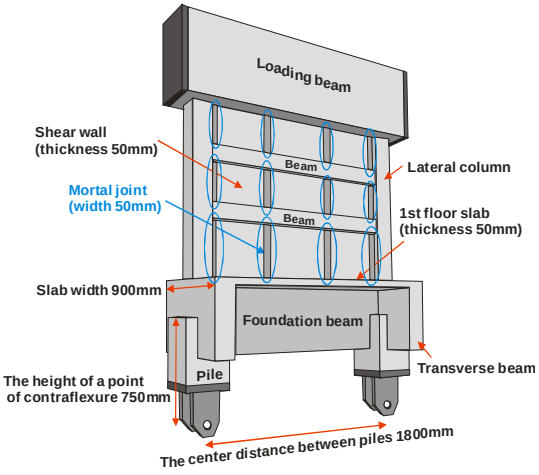

Fig.9 Perspective View of the Specimen

(2) Experiment and Analysis

Two test specimens which represent the bottom 3 stories of a typical 20 storey apartment house building were constructed and tested under quasi-static seismic loading. For the first one specimen, the concrete for the structural walls was monolithically cast and, for the second specimen, three precast concrete wall panels were provided for each story without shear keys and dowel reinforcement (see Figs.9 to 11). The nominal strengths of concrete and reinforcing steel are about

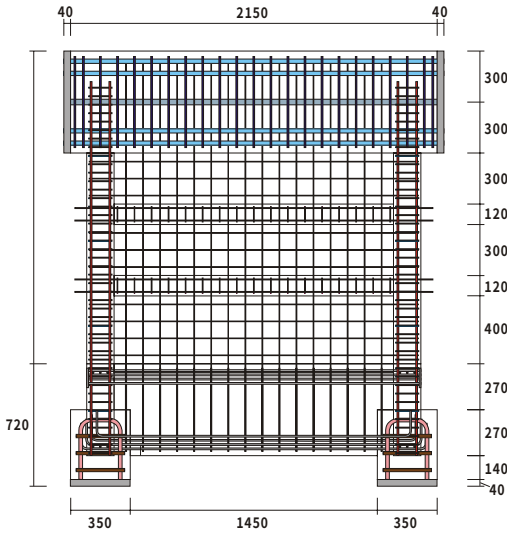

Fig.10 Reinforcing Details

40N/mm^2 and 300 to 400N/mm^2 , respectively. The Shear Force- Drift Angle Relationships shown in Figs.12 (a) and (b) indicated that the precast wall panels inserted to the system (or infill system) had satisfactory results. Figs. 13 and 14 indicate the observed crack pattern and the predicted crack pattern by FEM analysis.

They are indicating quite similar crack patterns and hence it may be concluded that the FEM models developed in this study are adequate.

(3) Conclusions

Old reinforced concrete frame structures which do not satisfy the current seismic design requirements can be satisfactorily retrofitted by inserting precast concrete wall panels. It was not necessary to provide shear keys or dowel reinforcement.

The FEM analytical model developed in this study could satisfactorily predicted the seismic behavior of the specimens tested in this project.

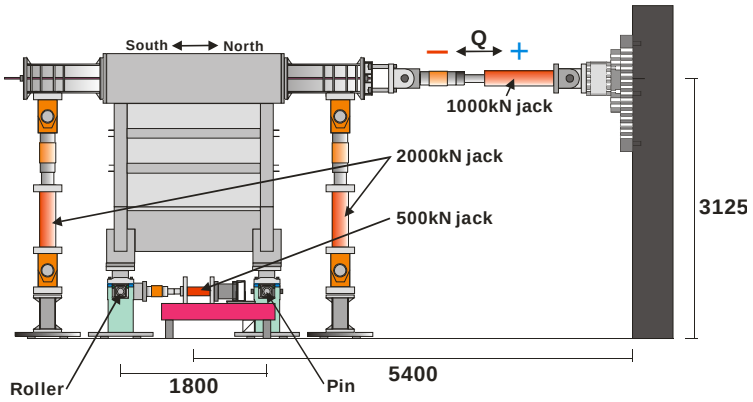

Fig.11 Loading System

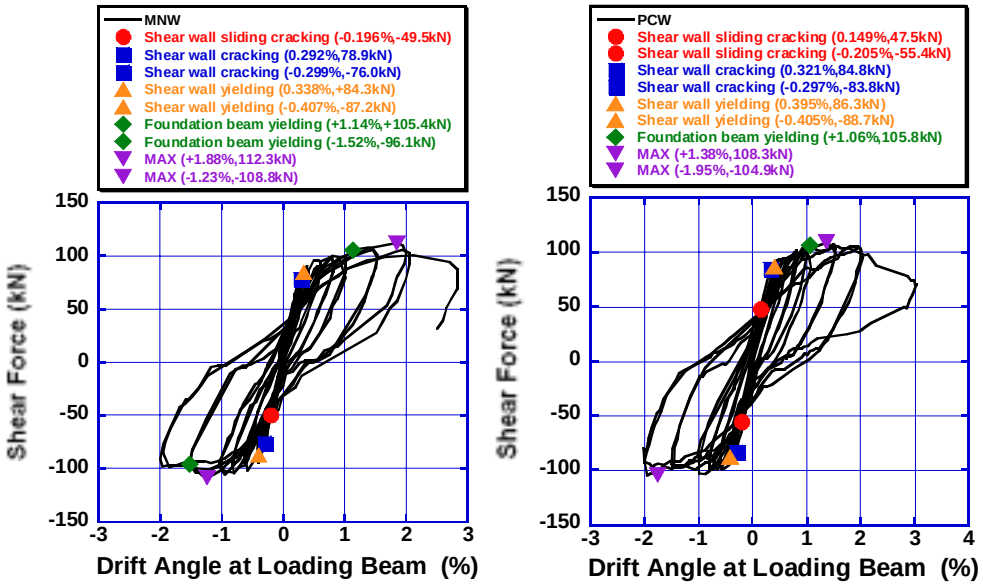

(a) (b)

Fig.12 Shear Force- Drift Angle Relationship;(a) Monolithic Concrete Wall, (b) Precast Concrete Wall with Vertical Slits

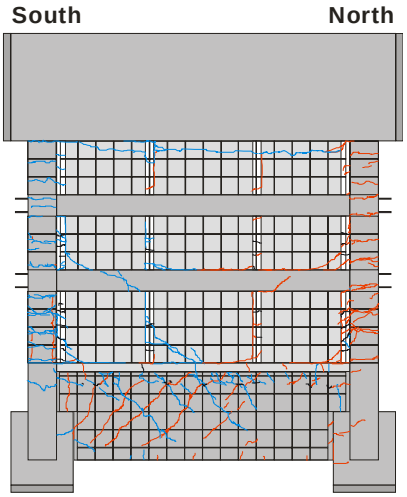

Fig. 13 Observed Crack Pattern

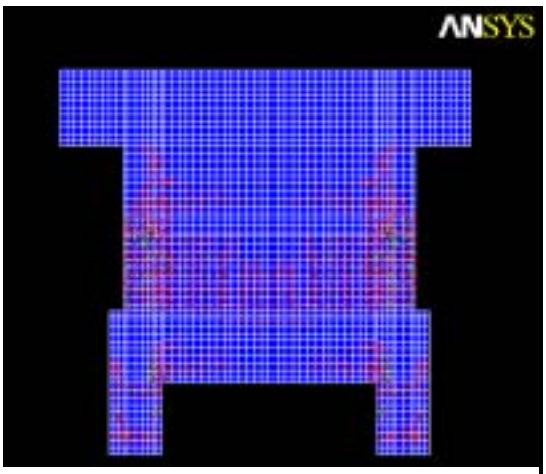

Fig.14 Crack Pattern Predicted by FEM Analysis

4. Prioritization of Seismic Reinforcement for Road Bridges-Based on the Concept of Life Cycle Cost

4.1 Introduction

Public structures are expected to perform their safety and continuous service of their intended function throughout their planned life time, with only acceptable probability of performance interruption or damage due to earthquakes. Therefore the structures lacking sufficient performance to earthquakes need to be reinforced. On the other hand, the budget for public project is curtailed year after year. Reinforcement works must be optimized efficiently under the constraint of a limited budget.

Risk due to earthquakes can be reduced by

strengthening existing structures and improving their ductility (Takahashi et al., 2002). To decide a strategy for reinforcement of existing structures, we should consider not only the cost of reinforcement but also the risk reduction. For this purpose we use a concept of 'Life Cycle Cost (LCC)'. LCC is defined as the expected total cost during a planned service time of a structure which include the costs of plan, design, construction, maintenance, repair and dismantlement (Frangopol et al., 1997).

It is important to prioritize the seismic reinforcement of several existing structures, which have different service time, and different level of importance considering both the initial cost and the risk reduction to earthquakes. In this paper, we pay attention to the difference between the structures' LCC of pre-reinforcement and post-reinforcement (defined as DLCC). A structure with large value of DLCC should be given a high priority to be reinforced because to reinforce such a structure is more cost-effective from the stand point of LCC.

We propose a methodology to prioritize the seismic reinforcement of several existing structures, which have different service time taking into account the deterioration with age. This methodology is applied to actual road bridges and evaluated its applicability.

4.2 Life Cycle Cost in Earthquake-resistant Design

The concept of DLCC defined by the difference of LCC (between pre-reinforcement and post -reinforcement) is used to prioritize the seismic reinforcement of existing structures. The priority of reinforcement is placed on structures with large DLCC. In general, LCC is defined by

$$C_{ET} = C_I + C_{PM} + C_{INS} + C_{REP} + C_F \qquad (1)$$

where C_{ET} is the expected total cost (LCC), C_I the initial cost, C_{PM} the expected cost of routine maintenance, C_{INS} the expected cost of inspection and repair maintenance, C_{REP} the cost of repair, and C_F the expected cost of failure. In this paper, we don't include the cost of maintenance in LCC because we pay attention only to the improvement of LCC by reinforcement. We define LCC by

$$LCC = C_I + \sum_{i=1}^{N} P_{fi} C_{fi} \qquad (2)$$

where C_I is the cost of reinforcement, P_{fi} the probability of damage due to earthquakes and C_{fi} the expected cost of damage. $\sum_{i=1}^{N} P_{fi} C_{fi}$ represents risk due to earthquakes. Even if the cost of reinforcement is expensive, decreasing risk caused by earthquakes makes LCC small.

The DLCC is defined as the effect of reinforcement by the following equation.

$$DLCC = LCC_0 - LCC_R$$

$$= (\sum_{i=1}^{N_0} P_{fi}^0 C_{fi}^0) - (C_R + \sum_{i=1}^{N_R} P_{fi}^R C_{fi}^R \quad (3)$$

where P_{fi}^0 is the probability of damage without reinforcement, C_{fi}^0 the expected cost of damage without reinforcement, N_0 the number of components expected to fail without reinforcement, P_{fi}^R the probability of damage with reinforcement, C_{fi}^R the expected cost of damage even with reinforcement, N_R the number of components expected to fail with reinforcement, and C_R the cost of reinforcement. We assign a high priority of reinforcement to the structure with a large DLCC.

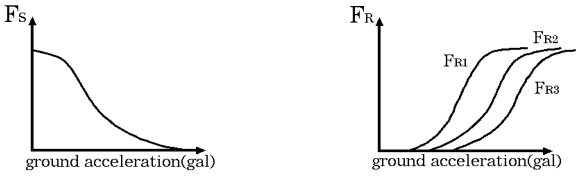

$$P_f = \int_0^{\infty} F_R(a) \frac{dF_s(a)}{da} da$$

Fig.15 : Image of seismic hazard curve (left) and fragility curve asfunction of peak ground acceleration

The important factor, which has a decisive influence on the risk to structures due to earthquakes, is the probability of damage. The probability of

damage to a structure due to earthquakes is given by numerical integration.

$$P_f = \int_0^\infty F_R(a) \frac{dF_s(a)}{da} da \qquad (4)$$

where $F_S(a)$ is the annual exceedance probability of a given level of seismic parameter for which the peak ground acceleration is used in this paper for a simplicity, and is called 'seismic hazard curve'. $F_R(a)$ is the conditional probability of the structure failure for a given level of seismic parameter, typically the peak ground acceleration and is called 'fragility curve'.

Seismic hazard curve represents the relation between seismic parameter and the annual exceedance probability at a concerned area. Based on historical data, we model activities of seismic source using a Poisson model or a non-Poisson renewal model. The Poisson model is adequate for earthquakes that frequently occur during the lifetime of the structures. However, for infrequent earthquakes, non-Poisson renewal model may be more appropriate. Recently, one renewal model, the Brownian Passage Time (BPT) model, has been applied to long-term estimation of earthquake probabilities (HERT, 2001). The Brownian motion with a drift is able to simulate accumulation of stress or strain of crust around the rupture plane. The BPT model can be expressed as the probability density function of interval time between successive renewals,

$$f(t) = \sqrt{\frac{\mu}{2\alpha^2 t^3}} \exp\left\{-\frac{(t-\mu)^2}{2\mu\alpha^2 t}\right\} \qquad (5)$$

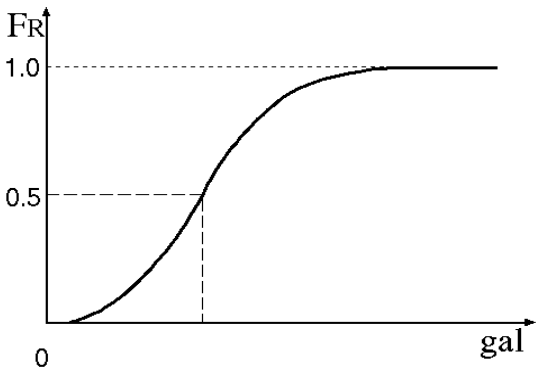

Fig.16 : Image of median

where *t* is a random variable standing for the interval time, μ the mean and α is the aperiodicity(=coefficient of variance).

The seismic fragility curve of a structural component is defined as the conditional probability of its failure for a given level of seismic parameter, typically the peak ground acceleration. Properly speaking, reliability analysis such as Monte Carlo simulation should be done considering uncertainties such as structural properties, ground properties and so on. In this paper, however, we compose the fragility curve using its median and coefficient of variance. The median is the probability of structural failure being 50%. We also assume that the gradient of the fragility curve does not have much effect on the probability of damage. The fragility curve is throughout assumed to be defined by a cumulative distribution function of lognormal distribution (Suwa *et al.*, 2001).

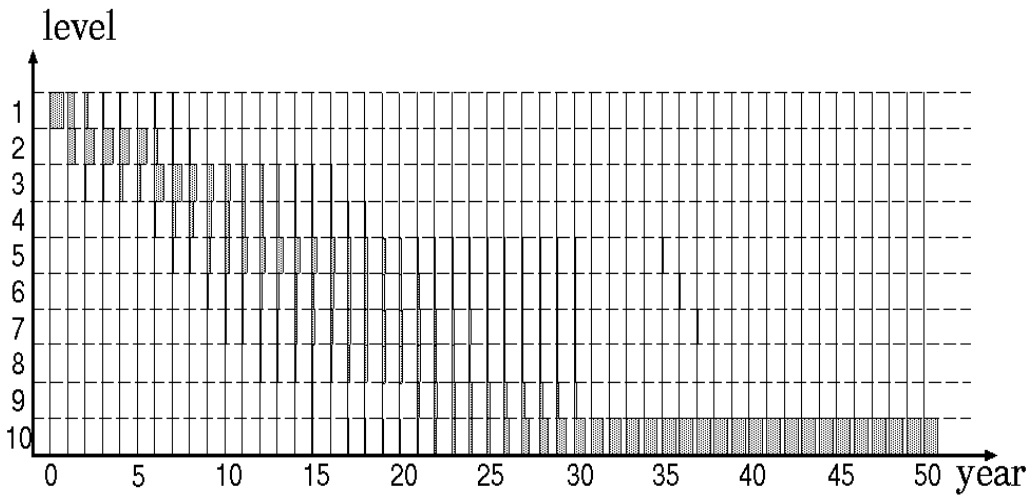

Fig. 17 : Deterioration model obtained from maintenance data of the bridge

$$F_R(a) = \Phi\left(\frac{\ln a - \lambda_R}{\zeta_R}\right) \quad (6)$$

where a is the seismic parameter (the peak ground acceleration), $\Phi(x)$ is the cumulative distribution functions of the normal distributions about x, λ_R is defined by,

$\lambda_R = \ln x_m$, x_m the median of x, and $\zeta_R^2 = 1 + \delta^2$, in which δ is coefficient of variance.

In this paper, we assumed that the minimum intensity of earthquake motion which causes damage to the structure is equivalent to the median of fragility curve. From this assumption the peak acceleration where safety factor becomes 1.0 obtained through dynamic analyses is assigned as the median.

If we have to consider several damage levels, the fragility curve for each level must be defined by calculating the median for each damage level.

When we prioritize the seismic reinforcement of structures based on the concept of Life Cycle Cost, we need to estimate not only the cost of reinforcement but also the cost of the object damaged due to earthquakes.

We use the estimated construction price as the cost of reinforcement. And the cost of damage is defined as

$$(C_{RE} + C_{TC}) \times a \times k \quad (7)$$

where C_{RE} is the cost of reconstruction, C_{TC} the cost of traffic control, a coefficient of importance (here we defined proportional to the volume of traffic) for each structure, and k scale factor. It is very difficult to estimate influence of the earthquake damage to structures upon surrounding society. So we consider influence of damage to structures upon surrounding society for prioritization by changing 'k'.

4.3 Model of Deterioration

As the structures deteriorate with age, their bearing capacities decrease. It is important to treat deterioration as stochastic process and to evaluate the probability of damage to structures taking into account the effect of deterioration.

The deterioration process is assumed to be expressed by a Markov chain in which the future condition of structures is assumed to depend only on the present state and independent on the past state (Zayed *et al.*, 2002). Knowing the present state of structure, or the initial state, the future conditions can be predicted through the multiplication of initial state vector and the transition probability matrix.

$$\mathbf{S}(t) = \mathbf{S}(t-1) \cdot \mathbf{P} \quad (8)$$

where $\mathbf{S}(t)$ is a state vector which consist of the probability that the condition lies in state k at time t, and $\mathbf{P}$ is the transition probability matrix. They can be written as

$$\mathbf{S}(t) = \{s(1,t) \quad s(2,t) \quad s(3,t) \quad \cdots \quad s(m,t)\} \quad (9)$$

where m is the number of deterioration levels.

$$\mathbf{P} = \begin{bmatrix} p_{11} & p_{12} & p_{13} & \cdot & \\ \cdot & p_{22} & p_{23} & p_{24} & \cdot \\ & \cdot & p_{33} & p_{34} & p_{35} \quad \cdot \\ & & \cdot & \cdot & \cdot \\ & & & & \end{bmatrix} \quad (10)$$

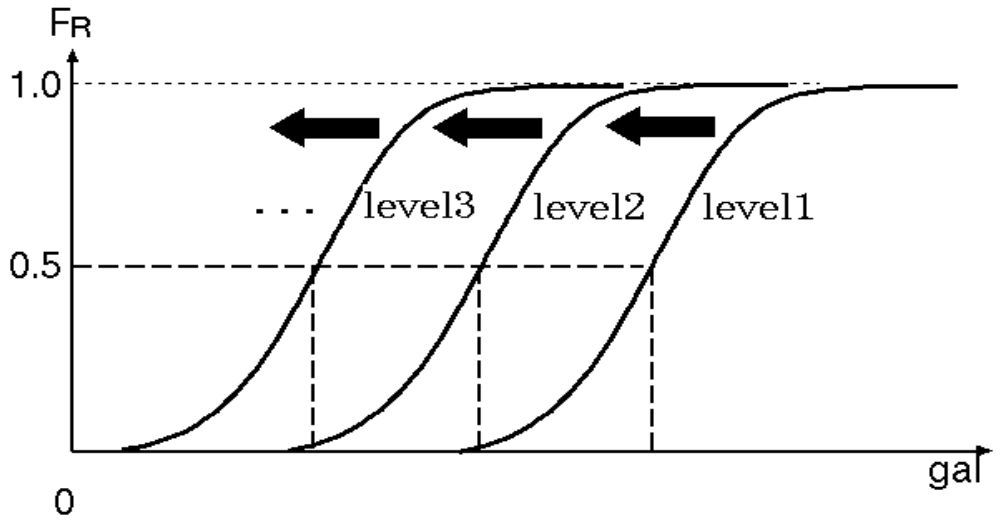

Fig. 18 : Image of shift of the fragility curve due to the deterioration of structural component

To estimate the transition probability matrix, we use a nonlinear programming approach. Due to the large amount of data and complexity of applying the Markov chain process to available data, the mean and variance of aging process are used. Then, the objective function of nonlinear program minimizes the square difference between the observed mean condition level at time t and the estimated mean condition level using a Markov chain at time t plus the square difference between the variance of the data at time t and the estimated variance of condition level using a Markov chain at time t. And the structure life is divided into several age periods within which a constant rate of deterioration is assumed.

The objective function to determine the transition probability matrix has the following form

Minimize

$$\sum_{i=1}^{N}\left\{\{Y(t)-E(t,\mathbf{P})\}^2+\left\{\sqrt{\sigma(t)^2}-\sqrt{V(t,\mathbf{P})}\right\}^2\right\}$$

$$\text{s.t.}\quad 0\le p(i)\le 1.0 \qquad (11)$$

where N is the number of years in one age period, $Y(t)$ the mean condition level at time t, E(t, **P**) the estimated value of condition level by Markov chains at time t, $\sigma(t)^2$ the variance obtained from the data, and V(t, **P**) the estimated variance of condition level using a Markov chain.

Fig. 17 shows the deterioration model obtained from the maintenance data of the bridge support (JSBC, 2000).

As the bearing capacity of structural element decreases, the fragility curve shifts to more dangerous side, left hand side as shown in Fig.18. We therefore evaluate the probability of structural damage for each deterioration level using the fragility curve corresponding to each deterioration level.

The annual probability of structural damage is estimated through the following steps.

1. Calculate fragility curves corresponding to each deterioration level.
2. Calculate the annual probability of damage corresponding to deterioration level k using the seismic hazard curve and the fragility curve corresponding to deterioration level k.
3. Because the deterioration condition is expressed by discrete random variable, the annual probability of structural damage at time t is obtained by the following form considering all possible deterioration level (Akaishizawa *et al.*, 2001).

$$P_{F(t)}=\sum_{k=1}^{m}p_f(k)\cdot s(k,t) \qquad (12)$$

$$\sum_{k=1}^{m}s(k,t)=1.0 \qquad (13)$$

where $P_F(t)$ is the annual probability of structural damage at time t to estimate LCC, $p_f(k,t)$ the annual probability of structural component damage corresponding to deterioration level k, *s(k , t)* the probability that thecondition lies in the state k at time *t*, and *m* the number of deterioration levels.

4.4 Application to actual road bridges

The methodology mentioned above is applied to prioritize the seismic reinforcement of actual 18 road bridges of Hanshin Expressway Public Corporation.

In this case study, the Uemachi Fault System (full lines in Fig.19) in Osaka is considered as a seismic source. The return period of this fault is estimated to be about 15000 years. In addition, it's not known exactly when the last event occurred. The annual occurrence rate is therefore assumed to be evaluated for applying the Poisson process.

$$\nu=1/15000=6.67\times10^{-5} \qquad (14)$$

The ground acceleration at the site of each concerned bridge is estimated by attenuation law. Because, we consider only one fault system, the seismic hazard curve represents the annual exceedance probability about the Uemachi Fault System. The variation of attenuation formula is regarded as lognormal distribution.

We classify 18 bridges into 5 groups based on their type. And we obtained the median of the fragility curves as functions of maximum acceleration at ground surface, for both pre-reinforcement and post-reinforcement conditions from dynamic response analyses of the representative bridge in each bridge group. We convert the median at the ground surface into the median at the engineering ground (shear wave velocity of 350m/s) using each ground model of surface layer at the site of concerned bridge based on the theory of one-dimensional multireflection. The fragility curve is defined for each bridge by a cumulative distribution function of lognormal distribution. Then we estimate the probability of damage by numerical integration. The cost of reinforcement and the cost of damage is calculated for each bridge. So we can estimate LCC without reinforcement (LCC_0) and LCC with reinforcement (LCC_R). And then DLCC (Eq. 3) can be obtained for each bridge.

Prioritization of seismic reinforcement bridges based on DLCC is conducted following three cases.

.case1:Changing coefficient of variance of the fragility curve.

.case2:Changing scale factor of the damage cost.

.case3:Comparing the prioritization result considering deterioration and the prioritization result not considering deterioration

In case1, there are minor alteration of prioritization due to the change of coefficient of variance of the fragility curve but there is not so much influence overall trend. In case2, there is not so much influence overall trend of prioritization. Now we consider the same scale factor for all concerned bridges. To estimate indirect influence of bridge damage, we have to take into account a factor reflecting the scale of the economic activity of surrounding area of a concerned bridge. In case3, there are alterations of prioritization. The rank of prioritization of old bridges sometimes goes up (Table 1). It is therefore important to consider the structural deterioration with age to prioritize the seismic reinforcement of existing structures, which have different service time.

4.5 Conclusions

We proposed a methodology for decision making of prioritization of seismic reinforcement of structural systems based on the concept of the difference of Life Cycle Cost (DLCC) taking into account of seismic risk. In the application to actual bridges, the applicability of this methodology is evaluated. Although there are many things we could not take into account to determine absolute prioritization, we can show overall trend. And we showed the importance to consider the structural deterioration with age.

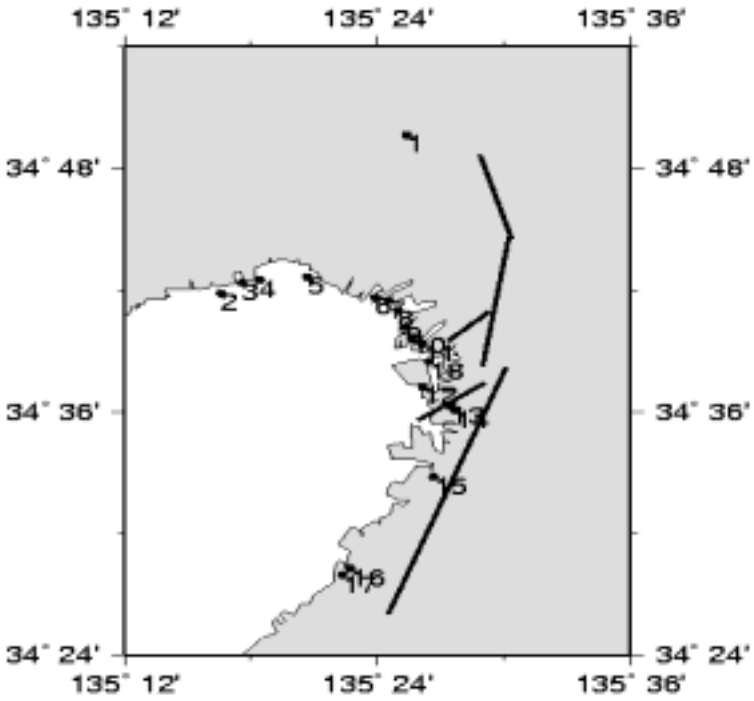

Fig. 19 : The Uemachi Fault System and bridge locations in the concerned area (each number shows bridge location)

Table 2 : Comparing the prioritization of reinforcement for the case considering deterioration with the case without considering

not considering

	No	t	LCC_0	LCC_R	DLCC
1	18	28	5072454.2	1369135.5	3703318.7
2	12	22	775316.6	191264.1	584052.5
3	15	9	271256.2	32369.4	238886.8
4	10	13	333753.3	102373.8	231379.5
5	8	12	261981.2	41176.0	220805.2
6	14	20	818927.2	604929.3	213997.9
7	11	14	665574.8	465745.1	199829.7
8	13	21	237051.5	47513.7	189537.7
9	7	11	150393.7	22292.6	128101.2
10	9	13	116529.7	14176.2	102353.5
11	17	10	112579.6	15402.8	97176.8
12	6	8	79254.4	7638.7	71615.7
13	5	8	69764.2	8218.2	61546.0
14	16	10	70121.3	9089.4	61031.9
15	4	8	45513.0	3755.3	41757.7
16	3	8	49753.0	18252.7	31500.3
17	1	4	34578.9	26335.6	8243.3
18	2	8	3310.8	3068.5	242.3

considering

	No	t	LCC_0	LCC_R	DLCC
1	18	28	5117285.3	1408094.2	3709191.1
2	12	22	775561.2	191264.1	584297.1
3	**10**	**13**	356256.9	102373.8	253883.2
4	**15**	**9**	271834.8	32369.4	239465.4
5	8	12	262878.2	41176.0	221702.2
6	14	20	819266.6	604929.3	214337.2
7	11	14	667187.3	465745.1	201442.2
8	13	21	238032.9	47513.7	190519.2
9	7	11	151567.7	22292.6	129275.2
10	9	13	117405.2	14176.2	103229.0
11	17	10	113234.2	15402.8	97831.4
12	6	8	81928.7	7638.7	74290.0
13	5	8	73042.9	8218.2	64824.7
14	16	10	70194.5	9089.4	61105.1
15	4	8	48605.5	3755.3	44850.1
16	3	8	57659.0	18252.7	39406.3
17	1	4	34698.7	26335.6	8363.0
18	2	8	3516.1	3068.5	447.6

(LCC and DLCC money unit : ten thousand yen)

No : the bridge number
t : the age of bridge

References

Asano, K., T. Iwata, and K. Irikura (2004): Estimation of the source rupture process and strong ground motion simulation of the 2002 Denali, Alaska, earthquake, in preparation for submitting Bull. Seism. Soc. Am.

Bouchon, M. (1997): The state of stress on some faults of the San Andreas system as inferred from near-field strong motions data, J. Geophysical Research, 102, 11731-11744.

Ikeda T, Kamae K, Miwa S, and Irikura K. (2002).: Source characterization and strong ground motion simulation of the 2000 Tottori-ken Seibu earthquake using the empirical Green's function method, Journal of Structural and Construction Engineering, Architectural Institute of Japan, 561, 37-45 (in Japanese with English abstract).

Irikura, K. and H. Miyake (2001): Prediction of strong ground motions for scenario earthquakes. Source model of the 1995 Hyogo-ken Nanbu earthquake and simulation of near-source ground motion, Journal of Geography, 110(6), 849-875 (in Japanese with English abstract).

Irikura, K., H. Miyake, T. Iwata, K. Kamae, H. Kawabe, and L. A. Dalguer (2003): Recipe for predicting strong ground motions for future earthquake, Ann. Disas. Prev. Res. Inst., Kyoto Univ., 46B, 105-120 (in Japanese with English abstract).

Iwata, T., H. Sekiguchi, H. Miyake, W. Zhang, and K. Miyakoshi (2004): Dynamic source parameters and characterized source model for strong motion prediction, Proc. 13th World Conf. Earthq. Eng., in printing.

Kamae K. and K. Irikura (1998): Source model of the 1995 Hyogo-ken Nanbu earthquake and simulation of near-source ground motion, Bulletin of the Seismological Society of America, 88(2), 400-412.

Kamae, K. and K. Irikura (2002). Source characterization and strong motion simulation for the 1999 Kocaeli, Turkey and the 1999 Chi-chi, Taiwan earthquakes, Proc. 11th Japan Conf. Earthq. Eng., 545-550 (in Japanese with English abstract).

Miyakoshi K, Kagawa T, Sekiguchi H, Iwata T, and Irikura K. (2000). Source characterization of inland earthquakes in Japan using source inversion results, Proceedings of the 12th World Conference on Earthquake Engineering, Auckland, New Zealand. Paper no. 1850. Upper Hutt, New Zealand: New Zealand Society for Earthquake Engineering.

Somerville, P. G., K. Irikura, R. Graves, S. Sawada, D. Wald , N. Abrahamson, Y. Iwasaki, T. Kagawa, N. Smith, and A. Kowada. (1999): Characterizing crustal earthquake slip models for the prediction of strong ground motion, Seismological Research Letters, 70(1), 59-80.

Yamada, N. and T. Iwata (2004): Long-period ground motion simulation in Kini area, Ann. Disas. Prev. Res. Inst., Kyoto Univ., 47C (in printing).

Zhang, W., T. Iwata, K. Irikura, H. Sekiguchi, and A. Pitarka (2003). Heterogeneous distribution of the dynamic source parameters of the 1999 Chi-Chi, Taiwan earthquake, J. Geophysical Research 2003; 108: 2232 doi: 10.1029/2002JB001889.

Akaishizawa, N., Yoshida, I., Yasuda, N., Miyamoto, K., (2001). “Optimization of Maintenance Frequency and Time for RC Structures based on Performance-Based Design.” *Journal of Structural Engineering*,, **47**(A), 227-290(in Japanese)

Frangopol, D. M., Lin, K-Y., Estes, A. C. (1997). “Life-Cycle Cost Design of Deteriorating Structures.” *Journal of Structural Engineering*, 123(10), 1390-1401

Headquarters for Earthquake Research Promotion (2001). *Evaluation Method and its Application for probability of Long-Term Earthquake Occurrence*,http://www.jishin.go.jp/main/choukihyoka/01b/index.htm (in Japanese)

Japan Association of Steel Bridge Construction (2000). *Life Cycle Cost of Steel Bridge* (in Japanese)

Suwa, H., Nobata, A., Seki, M., Wakamatsu, K., Suzuki, N., Mitsuhashi, E. (2001). “Seismic Risk Analysis for Buildings -Development of Software for Evaluating Probable Maximum Loss (PML)-.” *Report of Obayashi Corporation Technical Research Institute*, **63**, 61-66 (in Japanese)

Takahashi, Y., Kiureghian, A. D., Ang, A. H-S. (2002). “Decision Methodology in Seismic Risk Managemant of a Single Building Based on Minimum Expected Life-Cycle-Cost.” *the SEMM Report, Department of Civil & Environmental Engineering, University of California at Berkeley*, UCB/SEMM-2002.

Zayed, T. M., Chang, L-M., Fricker, J. D. (2002). ``Statewide Performance Function for Steel Bridge Protection Systems." *Journal of Performance of Constructed Facilitie*, **16**(2), 46-54

多次元評価指標の統合化による都市施設地震脆弱性診手法の高度化

佐藤忠信・入倉孝次郎・中島正愛・田中仁史・
松波孝治・澤田純男・吹田啓一郎・
岩田知孝・本田利器

要旨

都市域に存在する多くの構造物の地震時における脆弱性を合理的に評価するためには，構造物の共用期間，地震時に作用する外力，それに起因する被害コストや復旧にかかるコスト，さらには補強や維持管理にかかるコストも考慮に入れる必要があると考えられる．本研究では，このような点に鑑み，シナリオ地震による強震動予測や，ＲＣ構造物や鉄筋構造物の地震時被害のコントロールや，地震後に期待される構造物の残留強度，さらにはこれらを視野に入れたライフサイクルコストの評価を総合的に考慮できる手法の提案を試みた．

キーワード：強震動予測，特性化震源モデル，耐震性能評価，耐震補強，実大実験，
ライフサイクルコスト